

On Equation of State at physical quark masses

Peter Petreczky (for RBC-Bielefeld Collaboration) *[†]

Physics Department, Brookhaven National Laboratory, Upton NY 11973

E-mail: petreczk@bnl.gov

QCD equation of state are calculated in (2+1) flavor QCD at temperatures corresponding to the transition region with the physical values of the light quark masses using the p4 staggered fermion action on lattices with temporal extent $N_\tau = 8$. The results are compared with previous calculations performed at twice larger values of the light quark masses as well as with results obtained from the resonance gas model calculation. The deconfining and chiral aspects of the QCD transition are also discussed.

*The XXVII International Symposium on Lattice Field Theory
July 26-31, 2009
Peking University, Beijing, China*

*Speaker.

[†]This work has been supported by contract DE-AC02-98CH10886 with the U.S. Department of Energy. The numerical calculations have been performed using QCDOC supercomputers of USQCD Collaboration and RIKEN-BNL Research Center as well as the BlueGene/L at the New York Center for Computational Sciences (NYCCS).

1. Introduction

In the past five years a lot of progress has been achieved in calculating QCD Equation of State (for recent reviews see [1, 2, 3]). In the most recent calculations the Equation of State (EoS) has been evaluated for 2+1 flavor QCD, *i. e.* in QCD with one strange quark and two light (u, d) quarks using various improved staggered fermion actions [4, 5, 6, 7]. The most extensive calculations of the EoS have been performed with p4 and asqtad staggered fermion formulations on lattices with temporal extent $N_\tau = 4, 6$ [5, 6] and 8 [7]. These actions improve both the taste symmetry of the staggered fermions as well as the quark dispersion relations. The latter insures that thermodynamic observables are $\mathcal{O}(a^2)$ improved at high temperatures and thus have only a small cut-off dependence in this regime. The stout-link action, which has been used for the calculation of the EoS on lattices with temporal extent $N_\tau = 4, 6$ [4], only improves the taste symmetry of the staggered fermions and therefore has the same large discretization errors at high temperatures as the standard staggered fermion formulation. On the other hand the stout action has better taste symmetry which is important at low temperatures.

While at high temperatures the masses of the relevant degrees of freedom, quarks and gluons, are small compared to the temperature scale, this is not the case at low temperatures and in the transition region. One thus may expect that at these temperatures thermodynamic observables are more sensitive to the quark masses, which control the mass of the light pseudo-scalars and eventually are responsible for the occurrence of a true phase transition in the chiral limit. Calculations with p4 and asqtad actions have so-far been performed using light quark masses (m_l) which are one tenth of the strange quark mass (m_s) and correspond to a lightest pseudo-scalar Goldstone mass of 220 and 260 MeV respectively [7]. The calculations with the stout-link action have been performed at the physical value of the light quark mass.

The purpose of this work is to investigate the quark mass dependence of the EoS by calculating it with the p4-action for physical values of the (degenerate) light quark masses. The calculational procedure used in this work closely follows that used in our previous calculations at $\hat{m}_l = 0.1\hat{m}_s$ [6].

2. Calculations of the Equation of State

We have performed calculations with the p4-action for fourteen values of the gauge coupling $\beta = 6/g^2$ in the region of the finite temperature crossover. The finite temperature calculations have been performed on $32^3 \times 8$ lattices, while the corresponding zero temperature calculations have been performed on 32^4 lattices. We used the physical value for the strange quark mass and the ratio of strange to light quark mass was chosen to be $h = m_s/m_l = 20$. The lattice spacing was determined by calculating the static potential and extracting the Sommer scale r_0 from it. To remove the additive divergent constant in the potential following Ref. [6] we normalized it to the string potential $V_{string}(r) = -\pi/(12r) + \sigma r$ at distance $r = 1.5r_0$. This is needed for the renormalization of the Polyakov loop as discussed in Ref. [6]. In Figure 1 the static potential in units of r_0 and normalized to the string potential is shown. No discretization errors are visible in the potential. We extracted pseudo-scalar meson masses using wall sources in the calculation of meson propagators. It turned out that the η_{ss} mass is, with 1 -2 % accuracy, the same as in

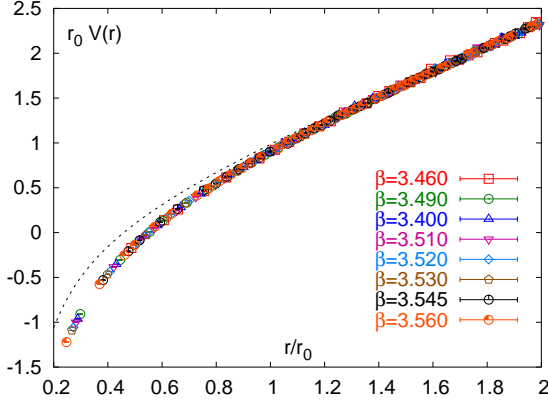


Figure 1: The static potential in units of r_0 calculated at different gauge couplings. The dashed line shows the string potential.

[6]. Thus, a re-adjustment of the line of constant physical $\eta_{s\bar{s}}$ mass corresponding to our new and smaller light quark masses was not necessary. In fact, in the present calculations we find that our quark mass values define a line of constant physics characterized by the following relations $r_0 \cdot m_\pi = 0.371(3)$, $r_0 \cdot m_K = 1.158(5)$, $r_0 \cdot m_{\eta_{s\bar{s}}} = 1.578(7)$ Using $r_0 = 0.469$ fm, as determined in Ref.[10], we get $m_\pi = 154$ MeV, $m_K = 486$ MeV and¹ $m_{\eta_{s\bar{s}}} = 663$ MeV. This means that both the light quark masses and the strange quark mass are very close to their physical values. Furthermore, in the entire parameter range covered by our thermodynamic calculations deviations of the meson masses from the above values are less than 3%.

The calculation of the EoS starts with the evaluation of the trace anomaly, *i.e.* the trace of the energy-momentum tensor $\Theta_{\mu\mu}(T)$. It is related to the temperature derivative of the pressure through thermodynamic identities,

$$\frac{\Theta_{\mu\mu}(T)}{T^4} = \frac{\varepsilon - 3p}{T^4} = T \frac{d}{dT} \left(\frac{p}{T^4} \right). \quad (2.1)$$

The trace anomaly can be expressed in terms of the expectation values of quark condensates and the gluon action density, see e.g. Ref. [7]. The numerical results are shown in Figure 2 and are compared to the previous calculation at twice larger quark mass $m_l = 0.1m_s$ on $N_\tau = 6$ lattices [6] and $N_\tau = 8$ lattices [7]. The differences between $N_\tau = 6$ and $N_\tau = 8$ calculations are due to cutoff effects and have been discussed in Ref. [7]. As one can see from the figure the main differences to the $N_\tau = 8$ results at $m_l = 0.1m_s$ arise for temperatures $T < 200$ MeV. These differences can be understood as resulting from an expected shift of the transition temperature by 5 MeV when the light quark mass is lowered to approximately its physical value. At lower temperatures it also is expected that the trace anomaly increases with decreasing quark masses as hadrons become lighter when the quark mass is decreased. While a tendency for such an increase may be indicated by the data at the lowest two temperatures reached in our calculation, this effect is certainly not significant within the current statistical accuracy.

¹A physical value for the $\eta_{s\bar{s}}$ mass can be obtained from the relation $m_{\eta_{s\bar{s}}} = \sqrt{2m_K^2 - m_\pi^2} = 686$ MeV.

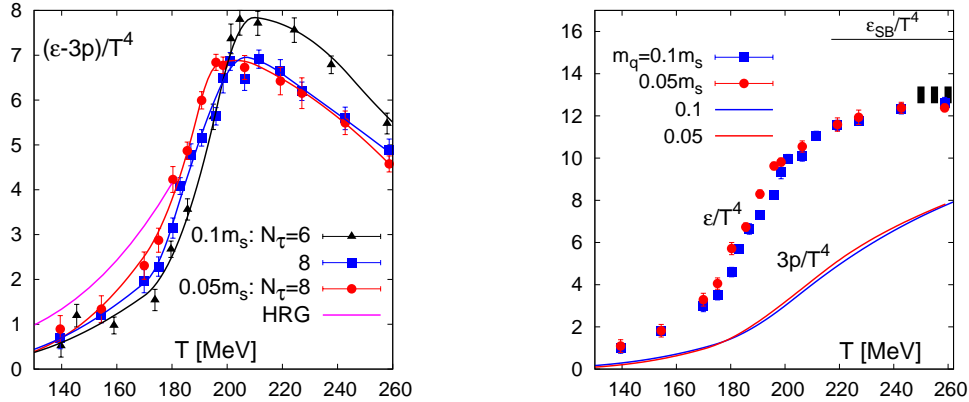


Figure 2: The trace anomaly $(\varepsilon - 3p)/T^4$ calculated for the physical quark mass and compared with previous calculations at larger light quark masses $m_l = 0.1m_s$ (left) and the pressure as well as the energy density (right). We compare the trace anomaly with as well as with the HRG model, which includes all the resonances up to 2.5GeV. The horizontal band shows the expected uncertainty in the energy density due to the choice of the lower integration limit

At temperatures below the transition temperature it is expected that thermodynamic quantities are well described by a hadron resonance gas (HRG) model. In fact, the freeze-out of hadrons in heavy ion experiments takes place in the transition region and the observed particle abundances are well described by the HRG model [12, 13]. Therefore in Figure 2 we also show the prediction of the HRG model, which includes all the known resonances up to the mass $M_{max} = 2.5$ GeV. The lattice data for $\varepsilon - 3p$ are below the HRG prediction although the deviations from it are smaller compared to the results obtained at $m_l = 0.1m_s$. We mention again the present statistical accuracy and the possibility of discretization effects in the hadron spectrum. In particular, due to taste breaking of staggered fermions pseudo-scalar mesons are not degenerate at finite lattice spacing, therefore their contribution to thermodynamic quantities may be suppressed.

From the trace anomaly the pressure and thus other thermodynamic quantities can be calculated by performing the integration over the temperature

$$\frac{p(T)}{T^4} - \frac{p(T_0)}{T_0^4} = \int_{T_0}^T dT' \frac{1}{T'^5} \Theta_{\mu\mu}(T'). \quad (2.2)$$

Here T_0 is an arbitrary temperature value that is usually chosen in the low temperature regime where the pressure and other thermodynamical quantities are suppressed exponentially by Boltzmann factors associated with the lightest hadronic states, i.e. the pions. Energy ε and entropy ($sT = (p + \varepsilon)$) densities are then obtained by combining results for p/T^4 and $(\varepsilon - 3p)/T^4$. The numerical results for the pressure and energy density are shown in Fig. 2. The uncertainties from the choice of the lower integration limit are shown as a horizontal band in the figure. The estimated uncertainties are about 8% in the energy density at the highest temperature of $T \simeq 260$ MeV, and about 13% for the pressure.

3. Deconfinement and chiral aspects of the QCD transition

In the previous section we have seen that the energy density shows a rapid rise in the tem-

perature interval $T = (170 - 200)\text{MeV}$. This is usually interpreted to be due to deconfinement, i.e. liberation of many new degrees of freedom. For sufficiently large quark mass this transition is known to be a first order transition (see e.g. Ref. [16]). In the limit of infinitely large quark mass the order parameter for the deconfinement phase transition is the Polyakov loop. After renormalization it can be related to the free energy of a static quark anti-quark pair $F_\infty(T)$ at infinite separation [17, 18] $L_{ren}(T) = \exp(-F_\infty(T)/(2T))$. A rapid change in this quantity is indicative for deconfinement also in the presence of light quarks. In the opposite limit of zero quark mass one expects a chiral transition and the corresponding order parameter is the chiral condensate. For a genuine phase transition, i.e. in the chiral limit the chiral condensate vanishes at the critical temperature T_c . However, we expect that even for the crossover at finite quark mass the light quark condensate rapidly drops in the transition region, indicating an approximate restoration of the chiral symmetry. At non-vanishing quark mass the chiral condensate needs additive and multiplicative renormalization. Therefore, following Ref. [6, 7] we introduce the so-called subtracted chiral condensate

$$\Delta_{l,s}(T) = \frac{\langle \bar{\psi}\psi \rangle_{l,\tau} - \frac{m_l}{m_s} \langle \bar{\psi}\psi \rangle_{s,\tau}}{\langle \bar{\psi}\psi \rangle_{l,0} - \frac{m_l}{m_s} \langle \bar{\psi}\psi \rangle_{s,0}}. \quad (3.1)$$

Here the subscripts l and s refer to light and strange chiral condensates, while the subscript 0 and τ to the case of zero and finite temperature respectively. Subtraction of the strange quark condensate multiplied by the ratio of the light to strange quark mass removes the quadratic divergence proportional to the quark mass.

In Figure 3 we show the renormalized Polyakov loop and the subtracted chiral condensate $\Delta_{l,s}$ and compare with previous calculations performed at light quark masses equal to one tenth of the strange quark mass [7]. The renormalized Polyakov loop rises in the temperature interval $T = (170 - 200)\text{ MeV}$ where we also see the rapid increase of the energy density. At the same time the subtracted chiral condensate rapidly drops in the transition region, indicating that the approximate restoration of the chiral symmetry happens in the same temperature interval as deconfinement. Compared to the calculation performed at light quark masses equal to one tenth of the strange quark mass we see a shift of the transition region by roughly 5 MeV. We note that such a shift arises differently in different observables. In the case of the subtracted chiral condensate, for instance, a major ingredient to the 'shift' is the fact, that at fixed temperature the condensate in the transition region is strongly quark mass dependent and drops proportional to $\sqrt{m_l/m_s}$ [19].

The fluctuation of strangeness is also indicative of deconfinement. It can be defined as the second derivative of the free energy density with respect to the strange quark chemical potential

$$\chi_s(T) = \frac{1}{T^3 V} \frac{\partial^2 \ln Z(T, \mu_s)}{\partial \mu_s^2} \Big|_{\mu_s=0}. \quad (3.2)$$

At low temperatures strangeness is carried by massive hadrons and therefore strangeness fluctuations are suppressed. At high temperatures strangeness is carried by quarks and the effect of the strange quark mass is small. Therefore strangeness fluctuations are not suppressed at high temperatures. As discussed in Ref. [7] strangeness fluctuations behave like the energy density in the transition region, i.e. they rapidly rise in a narrow temperature interval. In Fig. 4 we show the strangeness fluctuations calculated at $m_l = 0.05m_s$ and compare them with previous calculations performed at $m_l = 0.1m_s$ [7]. In the bottom figure we also show the strangeness fluctuation for

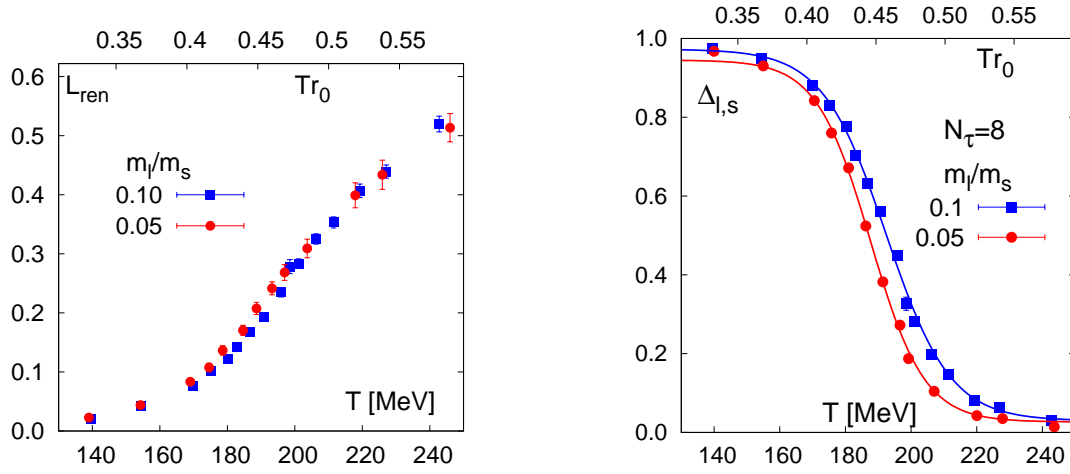


Figure 3: The renormalized Polyakov loop (left) and the subtracted chiral condensate (right) as function of the temperature calculated at $m_l = 0.05m_s$ and at $0.1m_s$.

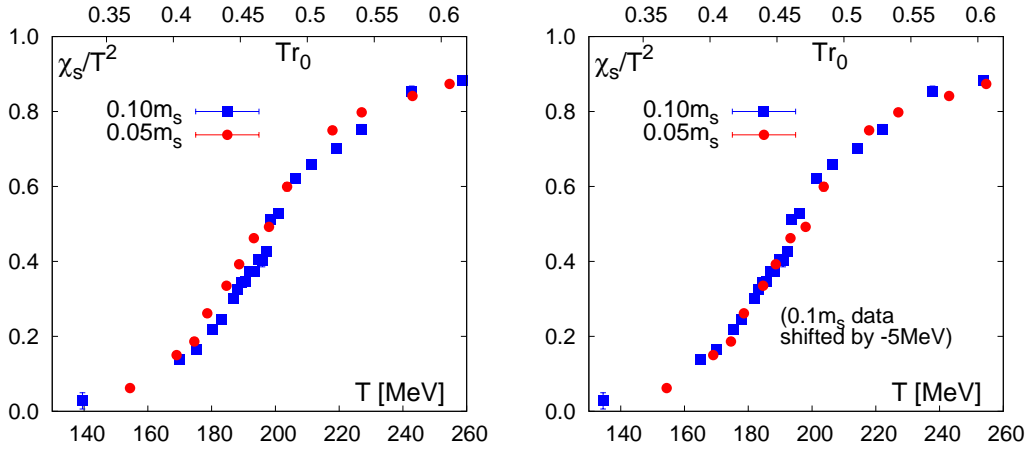


Figure 4: Strangeness fluctuations as function of the temperature calculated at $m_l = 0.05m_s$ and at $0.1m_s$. In the right plot the numerical data for $m_l = 0.1m_s$ have been shifted by 5 MeV.

$m_l = 0.1m_s$ with a 5 MeV shift of the temperature scale. As one can see this shift accounts for most of the quark mass dependence of the strangeness fluctuations. This is consistent with the conclusion obtained from the quark mass dependence of other thermodynamic observables.

4. Conclusion

We have calculated the EoS, renormalized Polyakov loop, subtracted chiral condensate and strangeness fluctuations in (2+1)-flavor QCD in the crossover region from low to high temperatures using the improved p4 staggered fermion formulation on lattices with temporal extent $N_\tau = 8$ at physical values of the light and strange quark masses. We found that thermodynamic quantities below the deconfinement transition are larger compared to the previous calculations performed at twice larger quark mass but fall below the resonance gas model result. The differences in the ther-

modynamic quantities calculated at $m_l = 0.05m_s$ and $m_l = 0.1m_s$ can be well understood in terms of the shift of the transition temperatures towards smaller values when the quark mass is decreased. This conclusion is also supported by the calculation of renormalized Polyakov loop, subtracted chiral condensate and strangeness fluctuations. No additional enhancement of the pressure and the energy density is seen at low temperatures. This and the deviation from the resonance gas model may be a cutoff effect due to taste violations. However, better statistical accuracy and calculations at smaller lattice spacing are needed to quantify this assertion. The transition region in our calculations corresponds to larger temperatures compared to recent calculations with stout action [20, 21]. It remains to be seen whether the taste symmetry violations which are larger for the p4 action are responsible for this discrepancy. At temperatures above 200 MeV no quark mass dependence is seen in the equation of state.

References

- [1] C. E. DeTar, PoS **LAT2008**, 001 (2008)
- [2] P. Petreczky, Nucl. Phys. A **785**, 10 (2007)
- [3] P. Petreczky, arXiv:0908.1917 [hep-ph].
- [4] Y. Aoki, Z. Fodor, S. D. Katz and K. K. Szabo, JHEP **0601**, 089 (2006)
- [5] C. Bernard *et al.*, Phys. Rev. D **75**, 094505 (2007).
- [6] M. Cheng *et al.*, Phys. Rev. D **77**, 014511 (2008).
- [7] A. Bazavov *et al.*, Phys. Rev. D **80**, 014504 (2009)
- [8] M. Cheng *et al.*, Eur. Phys. J. C **51**, 857 (2008).
- [9] M. Cheng *et al.*, Phys. Rev. D **74**, 054507 (2006)
- [10] A. Gray *et al.*, Phys. Rev. D **72**, 094507 (2005).
- [11] C. Allton, Nucl. Phys. B [Proc. Suppl.] **53**, 867 (1997)
- [12] J. Cleymans and K. Redlich, Phys. Rev. C **60**, 054908 (1999).
- [13] A. Andronic, P. Braun-Munzinger and J. Stachel, Nucl. Phys. A **772**, 167 (2006).
- [14] C. W. Bernard *et al.*, Phys. Rev. D **64**, 054506 (2001)
- [15] C. Aubin *et al.*, Phys. Rev. D **70**, 094505 (2004)
- [16] F. Karsch, C. Schmidt and S. Stickan, Comput. Phys. Commun. **147**, 451 (2002)
- [17] L.D.McLerran and B.Svetitsky, Phys. Rev. D **24** 450, (1981)
- [18] O. Kaczmarek, F. Karsch, P. Petreczky and F. Zantow, Phys. Lett. B **543**, 41 (2002)
- [19] S. Ejiri *et al.*, arXiv:0909.5122 [hep-lat].
- [20] Y. Aoki, Z. Fodor, S. D. Katz and K. K. Szabo, Phys. Lett. B **643**, 46 (2006)
- [21] Y. Aoki, S. Borsanyi, S. Durr, Z. Fodor, S. D. Katz, S. Krieg and K. K. Szabo, JHEP **0906**, 088 (2009)